

000 001 002 003 004 005 006 007 008 009 010 011 012 ESTIMATING LATENT REGULARIZATION PARAMETERS IN ILL-POSED PROBLEMS WITH SEMI-DEFINITE PRO- GRAMMING

013
014
015
016
017
018
019
020
021
022
023
024
025
026
027
028
029
030
031
032
033
034
035
036
037
038
039
Anonymous authors
Paper under double-blind review

ABSTRACT

013
014
015
016
017
018
019
020
021
022
023
024
025
026
027
028
029
030
031
032
033
034
035
036
037
038
039
Tikhonov smoothing is often used in estimation problems in ill-posed settings. In a variety of applications ranging from human-computer interaction to model explainability, it is important to retroactively estimate smoothing parameters from an already trained model. We introduce an inverse regularization problem – one that infers latent smoothing hyperparameters obtained from a trained model and its dataset; and show a fast and effective solution using semi-definite programming. The algorithm directly exploits the stationarity conditions of Tikhonov models to jointly recover the model parameter’s prior mean μ and Tikhonov precision matrix T from observed optimum θ^* . Our method formulates this as a multi-constraint least squares problem, providing a novel and interpretable approach. Empirically, our results show that our solution outperforms Bayesian approaches and solver-agnostic baselines on diverse benchmarks including diabetes, lung cancer, and California housing datasets.

1 INTRODUCTION

026
027
028
029
030
031
032
033
034
035
036
037
038
039
In machine learning, ill-posed problems arise when a model’s solution is not unique, lacks stability, or cannot be reliably determined from the available data, often leading to poor generalization and overfitting, e.g., a linear regression with more parameters than examples. Regularization addresses ill-posed problems in machine learning by adding a constraint or penalty to the loss function, which discourages overly complex models. Tikhonov regularizers, also known as ridge regularizers in machine learning, are a form of regularization that stabilize ill-posed problems by adding a penalty term to the loss function based on the ℓ_2 norm of the model parameters. In mathematical terms, consider the following linear model trained over a dataset $\{(x_i, y_i)\}_{i=1}^N$:

$$\theta^* = \arg \min_{\theta} \sum_{i=1}^N \phi(\theta^T x_i - y_i) + \lambda \|A(\theta - \mu)\|_2^2,$$

040
041
042
043
044
045
046
047
048
049
050
051
052
053
where ϕ is some convex and differentiable loss function and $T = A^T \cdot A$ is the Tikhonov regularization matrix. The problem above is a (T, μ) -regularized model, where these two hyperparameters aid in stabilizing the solution.

040
041
042
043
044
045
046
047
048
049
050
051
052
053
The Bayesian interpretation of this setup is the maximum a posteriori (MAP) estimate under a Gaussian prior on the model parameters, where the prior assumes θ^* is normally distributed around μ and with covariance $\Sigma = T^{-1} = (A^T A)^{-1}$ ($E[\theta^*] = \mu$ and $Cov[\theta^*] = \Sigma$). The regularization term corresponds to incorporating this prior belief into the training process, and thus, can be interpreted as an *inductive bias* or a prior belief in the probability of any certain final solution θ^* .

040
041
042
043
044
045
046
047
048
049
050
051
052
053
Normally, (T, μ) are given and the goal is to solve for θ^* . In a number of important settings, (T, μ) are *latent* – when some black-box modeling procedure produces a model with unknown or implicit regularization parameters. (T, μ) give us important insight into prior modeling beliefs. Therefore, retroactive inference of these parameters can be very valuable.

Example 1 Consider a panel of clinicians that are observing the results of a noisy clinical trial. They are given a scatter plot of dosage x and a noisy self-reported indicator of patient well-being

054 *y, and each is asked to draw a best-fit line relationship between the two based on their clinical*
 055 *experience. How do we characterize the latent prior belief in each clinician?*
 056

057 **Example 2** *Consider an LLM performing in-context learning where it classifies new examples pro-*
 058 *vided to it based on a few given examples. How do we characterize the inductive biases used to*
 059 *make these inferences from a small number of examples?*

060 **Example 3** *Consider a machine learning system where weights θ^* and a training dataset X, Y are*
 061 *known, however the provenance of θ^* is lost. The machine learning engineer would like to determine*
 062 *what optimization hyperparameters were likely used to derive θ^* for future training.*

063 Accordingly, we present a new estimation problem called *Inverse Regularization*. Given a model
 064 θ^* solved for a known loss function ϕ and a dataset X, Y , we attempt to infer the latent (T, μ) .
 065 For Example 1, this can be stated as “assuming the clinician are internally solving a least squares
 066 regression, what prior beliefs do they have about the relationship between X and Y ?” For Example
 067 2, this might be stated as “assuming that the LLM roughly behaves like a logistic regression, what
 068 prior beliefs do they have about the parameters?”. The inverse problem is a bit more complex than
 069 the forward problem that solves for the model parameters. We contribute a new algorithm that
 070 directly exploits the stationarity conditions to jointly recover the model parameter’s prior mean μ
 071 and Tikhonov precision matrix T from observed optimum θ^* . Our method formulates this as a
 072 multi-constraint least squares problem, providing a novel and interpretable approach.
 073

074 2 OUR CONTRIBUTION AND RELATED WORK

075 In many ML problems, the choice of the regularizer is decisive for both stability and interpretability
 076 of solutions. Classical Tikhonov methods assume a fixed structure for the precision matrix T (e.g.,
 077 identity, finite-difference Laplacian) and often set the prior mean $\mu = 0$. These assumptions are
 078 restrictive: they impose generic smoothness priors rather than data-adapted ones, and they fail to
 079 capture cases where meaningful prior information is embedded in a nonzero μ . In applications such
 080 as imaging, biomedical signal analysis, and causal time-series modeling, this mismatch can lead to
 081 biased reconstructions or loss of critical structure. A principled way to *recover* both T and μ directly
 082 from observations addresses this gap.
 083

084 Prior work to learning regularization has adopted multiple approaches of inferring the Tikhonov ma-
 085 trix which typically differ from our setting. Alberti et al. (2021) learn an optimal Tikhonov operator
 086 through risk minimization. Noschese & Reichel (2012) poses inverse matrix problems whose so-
 087 lutions produce application-adapted Tikhonov matrices. Bilevel methods Kunisch & Pock (2013);
 088 De los Reyes et al. (2017); Ehrhardt et al. (2023); Gazzola & Gholami (2024) tune regularization
 089 parameters indirectly via an outer loss. Bayesian methods Knapik et al. (2011); Bouriga & Féron
 090 (2011); Cho et al. (2020) estimate the prior covariance through hierarchical modeling, but usually
 091 assume a fixed or zero mean. Graph-based approaches Dong et al. (2016); Pavez & Ortega (2016)
 092 impose structural constraints such as Laplacian precision, rather than solving directly for T .
 093

094 Ng et al. (2000) introduce the ill-posed problem of Inverse Reinforcement Learning. They seek
 095 to infer the underlying reward function from the previously learned optimal policy. Their work
 096 shows how model behaviour can be explained through latent reward structures. Their resolution of
 097 non-uniqueness of solutions closely mimics the goal of inverse regularization.

098 In contrast, we formulate an *inverse regularization* problem that uses the stationarity condition

$$100 \quad 101 T(\theta^* - \mu) = b^*,$$

102 where (θ^*, b^*) are observed from the forward regularization problem. Our key contribution is to
 103 *jointly recover* the prior mean μ and the precision matrix T by solving a multi-constraint least
 104 squares system, extended with machine learning models to handle diverse priors. This provides a
 105 novel, direct route to an interpretable estimation of both prior mean and precision from observed
 106 optima.

107 Solving for T and μ is non-trivial. The stationarity condition provides only indirect information,
 108 and both T and μ are high-dimensional unknowns. Naive estimation may result in non-positive-
 109 definite T , instability due to ill-conditioning, or overfitting when multiple solutions exist. Bayesian

108 approaches handle uncertainty but are computationally expensive and often assume restrictive priors.
 109 Bilevel and risk-minimization approaches require large amounts of training data and do not directly
 110 tie to the optimality equations. Our formulation addresses these challenges by casting the problem as
 111 a multi-constraint least squares system, leveraging observed optimum (θ^*, b^*) and machine learning
 112 models to stabilize recovery.

113 The ability to recover an interpretable prior mean and precision has broad implications. In imaging,
 114 this enables data-driven reconstruction methods that adapt to underlying structures while remaining
 115 explainable. In healthcare time-series, it provides a way to learn clinically meaningful prior base-
 116 lines (μ) and structured dependencies (T) from observed dynamics, improving both prediction and
 117 causal interpretability. In general scientific computing, recovering T and μ offers a bridge between
 118 purely data-driven methods and mechanistic priors, allowing practitioners to integrate observed out-
 119 comes with interpretable regularizers. Thus, our framework not only advances the mathematical
 120 foundations of inverse regularization but also provides practical tools for high-impact domains.

121

122 3 PROBLEM STATEMENT

123

124 In this section, we describe the inverse regularization problem. We will focus on the least squares
 125 loss $\phi(y - \theta^T x) = \|y - \theta^T x\|_2^2$, but the techniques easily generalize to many other typically used
 126 loss functions including hinge loss, logistic loss, and ℓ_1 losses as well.

127

128 The standard approach to Linear Regression is to use ordinary least squares (OLS). However, when
 129 the problem is ill-posed (no unique solution – none or many) we can employ regularization – an
 130 ML technique that allows for an optimal trade-off between model complexity (bias) and out-of-
 131 sample performance (variance). We focus on Ridge regularization and its generalization – Tikhonov
 132 regularization.

133

134 Here, we solve a stabilized least-squares problem of the form:

$$135 \theta^* = \arg \min_{\theta} \sum_{i=1}^N \|\theta^T x_i - y_i\|_2^2 + \|\alpha I \cdot \theta\|_2^2$$

136

137 This is done particularly when dealing with multi-collinearity across variables. This formulation can
 138 be generalized to:

$$139 \theta^* = \arg \min_{\theta} \sum_{i=1}^N \|\theta^T x_i - y_i\|_2^2 + \lambda \|A(\theta - \mu)\|_2^2,$$

141

142 The Tikhonov matrix $T = A^T \cdot A$ is a precision matrix, which can be interpreted as defining a prior
 143 belief over model parameters θ under a Bayesian lens.

144

145 **Solving the Forward Problem:** Given data matrix $X \in \mathbb{R}^{n \times d}$, target feature $y \in \mathbb{R}^n$, the known
 146 regularization matrix $A \in \mathbb{R}^{p \times d}$ (and as a result, known Tikhonov matrix $T \in \mathbb{R}^{d \times d}$), and the prior
 147 model parameter mean $\mu \in \mathbb{R}^d$, we can obtain the optimal solution:

$$148 \theta^* = \arg \min_{\theta} \sum_{i=1}^N \|X\theta^T - y\|_2^2 + \lambda \|A(\theta - \mu)\|_2^2, \quad (1)$$

149

150 To solve for θ , we take a partial derivative of equation 1 w.r.t. θ . This gives us the first-order optimal
 151 linear system:

$$152 \nabla \theta = 2X^T(X\theta - y) + 2\lambda A^T A(\theta - \mu) = 0 \\ 153 \implies (X^T X + \lambda A^T A) \theta = X^T y + \lambda A^T A \mu \quad (2)$$

154

Upon defining $T = \lambda A^T A \in \mathbb{R}^{d \times d}$, we get:

$$155 (X^T X + T) \theta = X^T y + T \mu \quad (3)$$

156

157 The LHS $X^T X + T$ is invertible when $\lambda > 0$ and A has full column rank Tibshirani. In this case,
 158 we get a unique solution:

$$159 \theta^* = (X^T X + T)^{-1} (X^T y + T \mu) \quad (4)$$

160

161 This could be achieved in two ways: via a closed-form solution approach or via an iterative algorithm
 162 like L-BFGS (quasi-Newton method) Berahas et al. (2016); Liu & Nocedal (1989) or SGD Amari
 163 (1993).

162 3.1 INVERSE REGULARIZATION PROBLEM
163164 Now, we are set up to describe the inverse regularization problem. We are given a modeling problem
165 defined by the following equation:

166
167
$$\theta^* = \arg \min_{\theta} \sum_{i=1}^N \|\theta^T x_i - y_i\|_2^2 + \lambda \|A(\theta - \mu)\|_2^2,$$

168
169

170 and we know θ^* , $\{(x_i, y_i)\}_{i=1}^N$. The objective is to infer the most likely $T = A^T A$ and μ used to
171 produce θ^* from the given data.172 The interpretation of this problem is most clear in an agentic context. Consider a black-boxy agent
173 that is only known to be applying a linear policy that is a function of state x_i . We know that the agent
174 derived its policy from a dataset of observations X, Y , but do not know exactly how it arrived at the
175 observed linear policy. Here, the inverse regularization problem infers the agent's latent optimization
176 parameters T, μ that best explain the observed θ^* assuming optimal behavior.177 **Q1. Does this apply to non-linear modeling?** If the agent's policy is known to be non-linear, we
178 can apply the problem above over locally linear fragments of the state-space. In other words, we can
179 resolve what the latent regularization parameters are in a local neighborhood.180 **Q2. How does this relate to explainability?** In many explainable AI techniques, the goal is to
181 present simple input-to-output relationships between examples and their predictions for human un-
182 derstanding. In contrast, inverse regularization links a model's behavior to its training data, namely,
183 how strong the inductive bias is in the modeling procedure. A weaker inductive bias means that the
184 model more directly optimizes a loss on the data, and a stronger bias means that the model is more
185 closely centered around μ ignoring other evidence.187 4 SOLVING INVERSE REGULARIZATION
188189 We now present our techniques for solving inverse regularization to estimate the model parameter
190 mean and the Tikhonov precision matrix in the case of regression (which, in-turn, gives us the mean-
191 centered covariance matrix). At a high-level, our approach inverts the regularization equations –
192 given the observed optimal solution and gradients, we recover the latent hyperparameters that could
193 have generated them. We present this as a constrained optimization problem where the precision
194 matrix is positive semi-definite (corresponds to a valid covariance matrix), and we infer the mean in
195 closed form. We propose two methods of solving inverse regularization:
196197 1. **Biconvex SDP** – Trace-minimizing SDP with closed-form μ update. Here, we alternate
198 between a T-step and a μ -step for the solver until convergence.
199 2. **Diverse Priors** – Recovery using diverse priors on μ . Here, we aim for recovery using d
200 diverse priors μ_j to produce d constraints.
201202 **Stationarity Conditions** For the regularized least-squares problem in equation 1, the first-order
203 optimality (stationarity) condition is obtained in equation 2 by setting the gradient of the objective
204 to zero. We rearrange equation 3 to obtain the following form:
205

206
$$T(\theta - \mu) = -X^T(X\theta - y)$$

207

208 For notational convenience, we define
209

210
$$b = T(\theta - \mu), \tag{5}$$

211

212 so that the stationarity condition in equation 3 is equivalently written as
213

214
$$b = -X^T(X\theta - y). \tag{6}$$

215

216 Equation 6 highlights that the regularization term $T(\theta - \mu)$ can be interpreted as balancing the
217 residual correlation $X^T(X\theta - y)$, thereby enforcing a trade-off between data fit and prior structure.
218 We elaborate our solution methods below.

216 4.1 METHOD 1: BICONVEX SDP
217

218 Our first proposed solution – **Biconvex SDP** is a bi-convex trace-minimizing semi-definite program-
219 ming solver, that jointly solves for T and μ in alternate steps. Our aim is to pick the lowest-trace
220 PSD solution that fits the constraint, while allowing for slack (noise).

221 We set μ_{est}^0 to a zero vector, providing a neutral prior from which the alternating updates refine T
222 and μ . We alternate between the 2 steps below until we reach a point of convergence.
223

- 224 • T-step (convex): For fixed μ_{est} at the $k + 1^{\text{th}}$ step, solve:

$$225 \quad T_{\text{est}}^{k+1} = \arg \min_{T_{\text{est}}, \mu_{\text{est}}} \text{trace}(T_{\text{est}}^k) + \rho \|T_{\text{est}}^k(\theta^* - \mu_{\text{est}}^k) - b^*\|_2^2$$

- 227 • μ -step (closed-form): For fixed T_{est} at the $k + 1^{\text{th}}$ step, solve:

$$228 \quad \mu_{\text{est}}^{k+1} = \arg \min_{\mu_{\text{est}}} \|T_{\text{est}}^{k+1}(\theta^* - \mu_{\text{est}}^k) - b^*\|_2^2 + \gamma \|\mu_{\text{est}}^k\|_2^2$$

231 While this method neatly solves a biconvex problem and respects stationarity constraints, it’s solu-
232 tion tends to a low-rank, under-determined T_{est} (often rank 1) that satisfies the constraint, that’s not
233 necessarily close to the ground-truth T_{true} . We thus, propose an alternate approach, which enhances
234 the solution such that we’re more correctly able to recover the original Tikhonov matrix and mean
235 (model identifiability).

236 4.2 METHOD 2: DIVERSE PRIORS
237

238 The second approach - recovery using **Diverse Priors** on μ addresses the identifiability issue by
239 introducing multiple, diverse prior means. With only one prior μ , the stationarity condition does
240 not uniquely determine T ; many PSD solutions can satisfy a single constraint. To resolve this
241 ambiguity and narrow down the scope, we choose a collection of priors $\{\mu_j\}_{j=1}^J$, each producing
242 a different forward solution θ_j and corresponding residual vector b_j ($J \geq d$) from an independent
243 stationarity equation. Stacking these relations yields a linear system of equations in T . When the
244 shifts $\{\theta_j - \mu_j\}$ span \mathbb{R}^d , the precision matrix T is uniquely identifiable in the noiseless case. This
245 method formalizes the intuition that diverse priors provide multiple “views” of the same operator,
246 enabling exact recovery where a single constraint is insufficient.

247 We start by choosing J diverse priors $\{\mu_j\}_{j=1}^J$. For each j , we solve the forward problem to obtain
248 θ_j and compute $b_j = -X^\top(X\theta_j - y)$. By stacking the constraints $T_{\text{obs}}(\theta_j - \mu_j) = b_j$, we define
249 the block matrices:

$$250 \quad V = [\theta_1 - \mu_1 \ \dots \ \theta_J - \mu_J] \in \mathbb{R}^{d \times J}, \quad B = [b_1 \ \dots \ b_J] \in \mathbb{R}^{d \times J}.$$

251 Then the constraints can be expressed the matrix equation:

$$252 \quad T_{\text{obs}} V = B. \quad (\text{B0})$$

254 We use L-BFGS (Quasi-Newton Constrained Residual Minimization) and sum-of-squares loss so
255 that the stationarity equation is exactly recovered. For exact recovery, if $\text{rank}(V) = d$ (thus $J \geq d$
256 and the columns of V span \mathbb{R}^d), then

$$257 \quad T_{\text{obs}} = B V^{-1} = B V^+,$$

258 where V^{-1} applies when V is invertible, and V^+ denotes the Moore–Penrose pseudo-inverse. In
259 the noisy setting (model mismatch), we can estimate T_{obs} via PSD-regularized least squares:

$$260 \quad \min_{T_{\text{obs}} \succeq 0} \|T_{\text{obs}} V - B\|_F^2 + \gamma \|T_{\text{obs}}\|_F^2 + \alpha \text{tr}(T_{\text{obs}})$$

262 Dropping the PSD constraint yields the closed form

$$263 \quad \tilde{T}_{\text{obs}} = B V^\top (V V^\top + \gamma I)^{-1}. \quad (\text{B3})$$

264 Since numerical solvers and pseudo-inverses may introduce asymmetry or small negative eigenval-
265 ues, we enforce the structural constraint $T \succeq 0$ by projecting onto the PSD cone. This is achieved
266 by eigen-decomposition and clipping:

$$267 \quad T_{\text{obs}}^{\text{sym}} = \frac{1}{2}(\tilde{T}_{\text{obs}} + \tilde{T}_{\text{obs}}^\top), \quad T_{\text{obs}}^{\text{hat}} = \Pi_{\succeq 0}(T_{\text{obs}}^{\text{sym}}),$$

268 where $\Pi_{\succeq 0}$ denotes projection to the PSD cone via eigenvalue thresholding. This guarantees that
269 the recovered operator is a valid Tikhonov precision matrix.

270

5 EXPERIMENTS

271
 272 In these experiments, we aim to verify the correctness of a reconstructed Tikhonov precision matrix
 273 and prior mean (via Inverse Regularization methods) by setting up a forward regularization process
 274 for regression a priori. We choose a fixed Tikhonov matrix and prior mean as the ground truth
 275 for the forward process, which we hope to reconstruct in the inverse process. We assume that the
 276 regularization matrix A has full column rank, the Tikhonov precision matrix T is a square matrix,
 277 and it isn't rank-deficient, as there are more observations than features in our datasets.
 278

279

5.1 PIPELINE

280
 281 **Phase 1: Ground Truth Generation** The ground truth Tikhonov precision T_{true} and prior mean
 282 μ_{true} are sampled from a Normal-Wishart prior, the conjugate family for Gaussian mean and precision.
 283 Let $Q \in \mathbb{R}^{p \times d}$ be a reference operator and hyperparameters: ridge strength $\lambda > 0$, degrees of
 284 freedom $\nu_0 \geq d$, mean prior strength $\kappa_0 > 0$, and mean center $m_0 \in \mathbb{R}^d$. The Wishart scale is
 285

$$\Sigma_0 = \frac{\lambda}{\nu_0} Q^\top Q,$$

286 so that $\mathbb{E}[T_{\text{true}}] = \lambda Q^\top Q$. We then draw
 287

$$T_{\text{true}} \sim \mathcal{W}(\nu_0, \Sigma_0), \quad \mu_{\text{true}} | T_{\text{true}} \sim \mathcal{N}(m_0, (\kappa_0 T_{\text{true}})^{-1}).$$

288 This ensures that T_{true} is PSD and that μ_{true} has scale consistent with its precision, providing realistic
 289 ground truth for the setting.
 290

291 **Phase 2: Forward Regularization** Here, the goal is to solve for optimum θ^* . The Forward
 292 Regularization step can be achieved in two ways – via a closed-form solution approach (equation 1),
 293 or via training an ML model with custom penalty via OLS (ordinary least squares). We choose to
 294 iteratively train a Machine Learning regressor model to obtain the optimal solution (equation 3).
 295

296 The regressor model M takes as input a standardized dataset $\{X, Y\}$ which is split it into train
 297 and test sets: $\{X_{\text{train}}, y_{\text{train}}\}$, $\{X_{\text{test}}, y_{\text{test}}\}$, known Tikhonov matrix $T_{\text{true}} = \lambda A_{\text{true}}^T A_{\text{true}} \in \mathbb{R}^d$, and
 298 apriori model parameter mean μ_{true} . Post model learning from the training data, it outputs its optimal
 299 solution θ^* .
 300

301 **Phase 3: Inverse Regularization** After the forward regularization phase, we reconstruct an esti-
 302 mate of both the Tikhonov matrix $T_{\text{est}} = A_{\text{est}}^T A_{\text{est}}$ and the prior mean μ_{est} , given X , y and θ^* .
 303

304 The inverse regularizer solver method takes as input, the standardized train and test datasets
 305 $\{X_{\text{train}}, y_{\text{train}}\}$, $\{X_{\text{test}}, y_{\text{test}}\}$, the optimal solution θ^* , and the stationarity constraints b^* . It's output is
 306 the estimated Tikhonov precision matrix $T_{\text{est}} = A_{\text{est}}^T A_{\text{est}} \in \mathbb{R}^d$, and the prior mean μ_{est} .
 307

308 We employ the following set of 10 techniques to solve inverse regularization:
 309

- 310 (a) **5 baselines:** {Identity Ridge, Diagonal Ridge, PSD LS Ridge, Zero Mean Ridge, Random SPD}
- 311 (b) **3 Bayesian benchmarks:** {MAP, MCMC, VI}
- 312 (c) **2 proposed methods (ours):** {Biconvex SDP, Diverse Priors}

313

5.2 METRICS OF EVALUATION

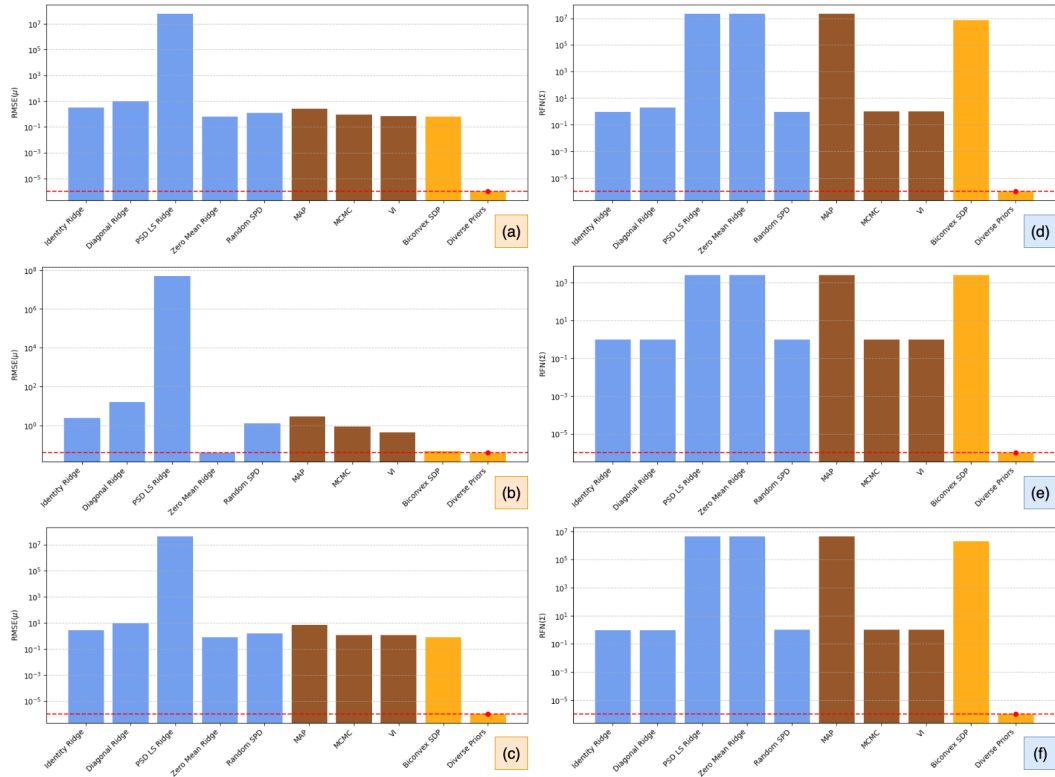
314 We present the following three metrics in our results: (i) the relative Frobenius error in the Tikhonov
 315 precision matrix – which measures how well the estimated precision matches the ground truth struc-
 316 ture; (ii) the mean error – quantifying accuracy in recovering the prior mean; and (iii) the relative
 317 Frobenius error in the covariance matrix – which evaluates recovery of uncertainty structure. To-
 318 gether, these metrics highlight fidelity to the underlying operator, accuracy of the estimated mean,
 319 and uncertainty in calibration.
 320

378
 379
 380
 381
 382

- California housing dataset: This dataset from the *sklearn* library consists of 21,000 individual data records and 8 fields. The goal is to predict the Median house value for California districts. https://scikit-learn.org/stable/modules/generated/sklearn.datasets.fetch_california_housing.html

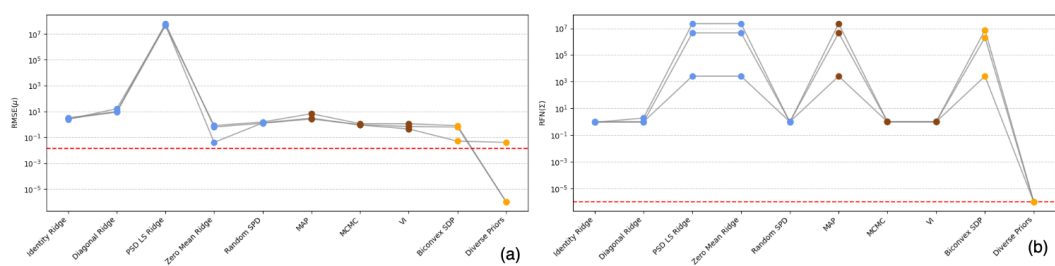
383 The above collection of datasets allows us to evaluate the performance of our methods in diverse
 384 settings. This allows for our work to be easily generalizable to other datasets (different distributions,
 385 causal priors), and other ML prediction tasks like classification.

386 We defer further implementation details and theory to the appendix.
 387



407
 408
 409
 410
 411
 412
 413
 414
 415
 416
 417
 418
 419
 420
 421
 422
 423
 424
 425
 426
 427
 428
 429
 430
 431

Figure 1: Left Column: Comparison of $RMSE(\mu)$ values and Right Column: Comparison of $RFN(\Sigma)$ across all techniques for the three datasets: (a),(d): Diabetes, (b),(e): Lung Cancer, and (c),(f): California Housing. The blue bars highlight the baselines, the brown ones - benchmarks, and the orange bars correspond to our methods.



430
 431
 432
 433
 434
 435
 436
 437
 438
 439
 440
 441
 442
 443
 444
 445
 446
 447
 448
 449
 450
 451
 452
 453
 454
 455
 456
 457
 458
 459
 460
 461
 462
 463
 464
 465
 466
 467
 468
 469
 470
 471
 472
 473
 474
 475
 476
 477
 478
 479
 480
 481
 482
 483
 484
 485
 486
 487
 488
 489
 490
 491
 492
 493
 494
 495
 496
 497
 498
 499
 500
 501
 502
 503
 504
 505
 506
 507
 508
 509
 510
 511
 512
 513
 514
 515
 516
 517
 518
 519
 520
 521
 522
 523
 524
 525
 526
 527
 528
 529
 530
 531
 532
 533
 534
 535
 536
 537
 538
 539
 540
 541
 542
 543
 544
 545
 546
 547
 548
 549
 550
 551
 552
 553
 554
 555
 556
 557
 558
 559
 560
 561
 562
 563
 564
 565
 566
 567
 568
 569
 570
 571
 572
 573
 574
 575
 576
 577
 578
 579
 580
 581
 582
 583
 584
 585
 586
 587
 588
 589
 590
 591
 592
 593
 594
 595
 596
 597
 598
 599
 600
 601
 602
 603
 604
 605
 606
 607
 608
 609
 610
 611
 612
 613
 614
 615
 616
 617
 618
 619
 620
 621
 622
 623
 624
 625
 626
 627
 628
 629
 630
 631
 632
 633
 634
 635
 636
 637
 638
 639
 640
 641
 642
 643
 644
 645
 646
 647
 648
 649
 650
 651
 652
 653
 654
 655
 656
 657
 658
 659
 660
 661
 662
 663
 664
 665
 666
 667
 668
 669
 670
 671
 672
 673
 674
 675
 676
 677
 678
 679
 680
 681
 682
 683
 684
 685
 686
 687
 688
 689
 690
 691
 692
 693
 694
 695
 696
 697
 698
 699
 700
 701
 702
 703
 704
 705
 706
 707
 708
 709
 710
 711
 712
 713
 714
 715
 716
 717
 718
 719
 720
 721
 722
 723
 724
 725
 726
 727
 728
 729
 730
 731
 732
 733
 734
 735
 736
 737
 738
 739
 740
 741
 742
 743
 744
 745
 746
 747
 748
 749
 750
 751
 752
 753
 754
 755
 756
 757
 758
 759
 760
 761
 762
 763
 764
 765
 766
 767
 768
 769
 770
 771
 772
 773
 774
 775
 776
 777
 778
 779
 780
 781
 782
 783
 784
 785
 786
 787
 788
 789
 790
 791
 792
 793
 794
 795
 796
 797
 798
 799
 800
 801
 802
 803
 804
 805
 806
 807
 808
 809
 810
 811
 812
 813
 814
 815
 816
 817
 818
 819
 820
 821
 822
 823
 824
 825
 826
 827
 828
 829
 830
 831
 832
 833
 834
 835
 836
 837
 838
 839
 840
 841
 842
 843
 844
 845
 846
 847
 848
 849
 850
 851
 852
 853
 854
 855
 856
 857
 858
 859
 860

Figure 2: (a): Comparison of avg. $RMSE(\mu)$ values and (b): Comparison of avg. $RFN(\Sigma)$ values across all techniques averaged over all datasets.

432 5.6 RESULTS & ANALYSIS
433

434
435 We evaluate both the proposed solutions against baselines and benchmarks for key recovery metrics:
436 RMSE of the recovered prior mean μ and Relative Frobenius Norm (RFN) error of the covariance
437 matrix (inverse of the Tikhonov precision matrix). Σ . Figures 1 and 2 summarize the empirical
438 findings. We show additional results on the RFN error of the recovered Tikhonov precision T in
439 the appendix. Figure 1 offers a comparison of the RMSE error of predicted means by the different
440 methods for the three datasets in bar plots (a), (b), and (c) respectively (left column). It also shows
441 a comparison of RFN error in the predicted covariance matrices in bar plots (d), (e), and (f) re-
442 spectively (right column). Figure 2 offers a similar comparison – RMSE(μ) and RFN(Σ), averaged
443 across the three datasets - to account for generalization.

444 From these plots we can see that baselines based on classical ridge regularizers (Identity, Diagonal,
445 PSD LS, and Zero Mean Ridge) and random SPD initializations perform poorly, often yielding
446 errors several orders of magnitude larger than the ground truth. In particular, PSD LS ridge exhibits
447 extreme instability, potentially because inversion of the ill-conditioned constraint matrix amplifies
448 noise, resulting in large errors in both mean and covariance recovery. Zero-mean ridge, on the other
449 hand, by fixing $\mu = 0$, forces the precision to absorb model mis-specification, making covariance
450 estimates particularly unstable. MAP, MCMC, and variational inference (VI) achieve moderate
451 performance, consistently outperforming naive baseline methods, but still incurring residual bias
452 and variance. MAP underperforms MCMC and VI because it returns only a single mode of the
453 posterior, ignoring uncertainty and multimodality. In contrast, MCMC and VI integrate over the
454 posterior, yielding relatively more robust estimates of both the mean and covariance.

455 Now we discuss the results of our approaches. As expected, the **Biconvex SDP** method doesn't
456 perform as well in recovering the covariance matrix because it prefers rank-deficient solutions. In
457 contrast, the **Diverse Priors** method improves upon Bayesian benchmarks across all datasets by
458 explicitly enforcing PSD structure and leveraging multiple independent constraints. It achieves near-
459 exact recovery, with RMSE(μ) and RFN(Σ) approaching numerical precision (dashed red line).
460 This yields full-rank, well-conditioned estimates of both the mean and covariance, achieving the
461 most accurate recovery overall. This validates the identifiability argument: multiple independent
462 prior means provide sufficient constraints to uniquely recover the Tikhonov operator. Additionally,
463 we observe the computational time for all methods. While all the baselines run in the order of a few
464 milliseconds and our proposed methods – Biconvex SDP and Diverse priors run under 1 second, and
465 the Bayesian approaches approximately require over a little over 1 hour to find a solution.

466 Overall, the results confirm that while traditional ridge and Bayesian approaches offer partial recov-
467 ery, they cannot guarantee identifiability. Our proposed method based on Diverse Priors consistently
468 outperforms alternatives, achieving exact recovery in the noiseless case and robust performance un-
469 der perturbations. Our approach brings a nuance to testing the strength of priors that can benefit our
470 understanding of ML models.

471 In the future, we plan on extending this work to classification models, and more smoothing priors –
472 such as the Graph Laplacian for causal datasets, and other application-specific kernel based priors.
473 We are also working on applying our work to enhance model explainability for tools like LIME
474 Ribeiro et al. (2016).

475
476 6 CONCLUSION
477

478
479
480 We present a new estimation problem called Inverse Regularization that infers latent smoothing hy-
481 perparameters obtained from a trained prediction model and its dataset. We propose the novel “Di-
482 verse Priors” method for jointly inferring the model parameters’ prior mean and Tikhonov precision
483 matrix. This solution makes use of semi-definite programming and the Tikhonov model’s stationar-
484 ity conditions. We formulate it as a unique and interpretable multi-constraint least squares problem.
485 Our proposed solution is fast and effective, and outperforms all baselines and Bayesian benchmarks
486 presented on diverse datasets, delivering state-of-the-art recovery of the model parameters.

486 7 ETHICS STATEMENT
487488 We confirm that our work adheres to ICLR’s code of ethics. Our work does not involve human
489 subjects, sensitive data, or applications that can cause societal harm. The datasets used (Diabetes,
490 Asia lung cancer, and California housing) are publicly available and widely adopted benchmarks.
491 Our methods are intended for improving understanding of regularization and inverse problems in
492 machine learning optimization, and do not raise any ethical concerns.493 We have made use of ChatGPT 5 specifically to aid with polishing writing at a grammatical level –
494 sanity checks in sentence construction, and finding the right synonyms for words.
495496 8 REPRODUCIBILITY STATEMENT
497498 We ensure reproducibility of our results. All datasets are standard and publicly available. Complete
499 algorithmic details, proofs, and hyperparameter settings are provided in the main text and appendix.
500 In addition, all code used to run the experiments is included in the supplementary materials.
501

502 503 REFERENCES

504 Giovanni S. Alberti, Ernesto De Vito, Matti Lassas, Luca Ratti, and Matteo Santacesaria. Learning
505 the optimal tikhonov regularizer for inverse problems, 2021. URL <https://arxiv.org/abs/2106.06513>.
506507 Shun-ichi Amari. Backpropagation and stochastic gradient descent method. *Neurocomputing*, 5
508 (4-5):185–196, 1993.509 Albert S Berahas, Jorge Nocedal, and Martin Takáć. A multi-batch l-bfgs method for machine
510 learning. *Advances in Neural Information Processing Systems*, 29, 2016.511 Mathilde Bouriga and Olivier Féron. Estimation of covariance matrices based on hierarchical
512 inverse-wishart priors, 2011. URL <https://arxiv.org/abs/1106.3203>.
513514 Taewon Cho, Julianne Chung, and Jiahua Jiang. Hybrid projection methods for large-scale in-
515 verse problems with mixed gaussian priors, 2020. URL <https://arxiv.org/abs/2003.13766>.
516517 Juan Carlos De los Reyes, C-B Schönlieb, and Tuomo Valkonen. Bilevel parameter learning for
518 higher-order total variation regularisation models. *Journal of Mathematical Imaging and Vision*,
519 57(1):1–25, 2017.520 Xiaowen Dong, Dorina Thanou, Pascal Frossard, and Pierre Vandergheynst. Learning laplacian
521 matrix in smooth graph signal representations. *IEEE Transactions on Signal Processing*, 64(23):
522 6160–6173, 2016.523 Matthias J Ehrhardt, Silvia Gazzola, and Sebastian J Scott. On optimal regularization parameters
524 via bilevel learning. 2023.525 Silvia Gazzola and Ali Gholami. Automatic nonstationary anisotropic tikhonov regularization
526 through bilevel optimization. *arXiv preprint arXiv:2406.02209*, 2024.527 Bartek T Knapik, Aad W Van Der Vaart, and J Harry van Zanten. Bayesian inverse problems with
528 gaussian priors. *The Annals of Statistics*, pp. 2626–2657, 2011.529 Karl Kunisch and Thomas Pock. A bilevel optimization approach for parameter learning in varia-
530 tional models. *SIAM Journal on Imaging Sciences*, 6(2):938–983, 2013.531 Dong C Liu and Jorge Nocedal. On the limited memory bfgs method for large scale optimization.
532 *Mathematical programming*, 45(1):503–528, 1989.533 Andrew Y Ng, Stuart Russell, et al. Algorithms for inverse reinforcement learning. In *Icml*, vol-
534 ume 1, pp. 2, 2000.

540 Silvia Noschese and Lothar Reichel. Inverse problems for regularization matrices. *Numerical Algo-*
 541 *rithms*, 60(4):531–544, 2012.
 542

543 Eduardo Pavez and Antonio Ortega. Generalized laplacian precision matrix estimation for graph
 544 signal processing. In *2016 IEEE International Conference on Acoustics, Speech and Signal Pro-*
 545 *cessing (ICASSP)*, pp. 6350–6354. IEEE, 2016.
 546

547 Marco Tulio Ribeiro, Sameer Singh, and Carlos Guestrin. ” why should i trust you?” explaining the
 548 predictions of any classifier. In *Proceedings of the 22nd ACM SIGKDD international conference*
 549 *on knowledge discovery and data mining*, pp. 1135–1144, 2016.
 550

551 Ryan Tibshirani. High-dimensional regression: Ridge.
 552

553 Chendong Zhang and Ting Chen. Bayesian slip inversion with automatic differentiation variational
 554 inference. *Geophysical Journal International*, 229(1):546–565, 2022.
 555

558 A APPENDIX

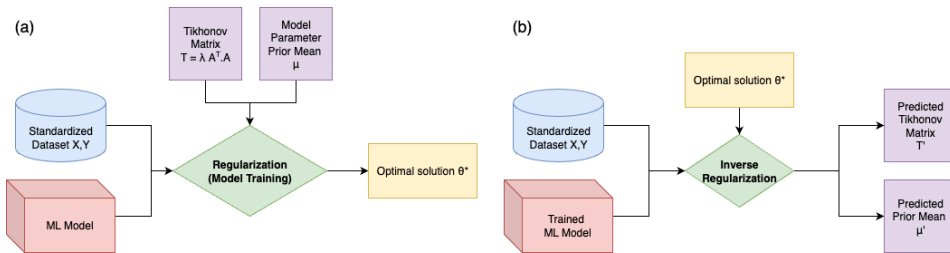
560 We share some additional details, plots, results, and theory in the appendix.
 561

563 A.1 ASIA LUNG CANCER RESULT

566 Table 1: Error Metrics for Asia Lung Cancer Dataset

568 Method	RFN(T)	RMSE(μ)	RFN(Σ)
569 Identity Ridge	0.92	2.40	1.00
570 Diagonal Ridge	0.99	16.38	1.00
571 PSD LS Ridge	0.94	4.91×10^7	2.61×10^3
572 Zero Mean Ridge	0.94	0.04	2.609×10^3
573 Random SPD	1.86	1.30	1.00
574 MAP	0.99	3.00	2.603×10^3
575 MCMC	3.08	0.88	1.00
576 VI	0.88	0.44	1.00
577 Biconvex SDP	0.86	0.05	2.608×10^3
578 Diverse Priors	1.0×10^{-3}	0.04	1.0×10^{-3}

581 A.2 PIPELINE FLOWCHART



593 Figure 3: Pipeline of (a) forward regularization and (b) inverse regularization.
 594

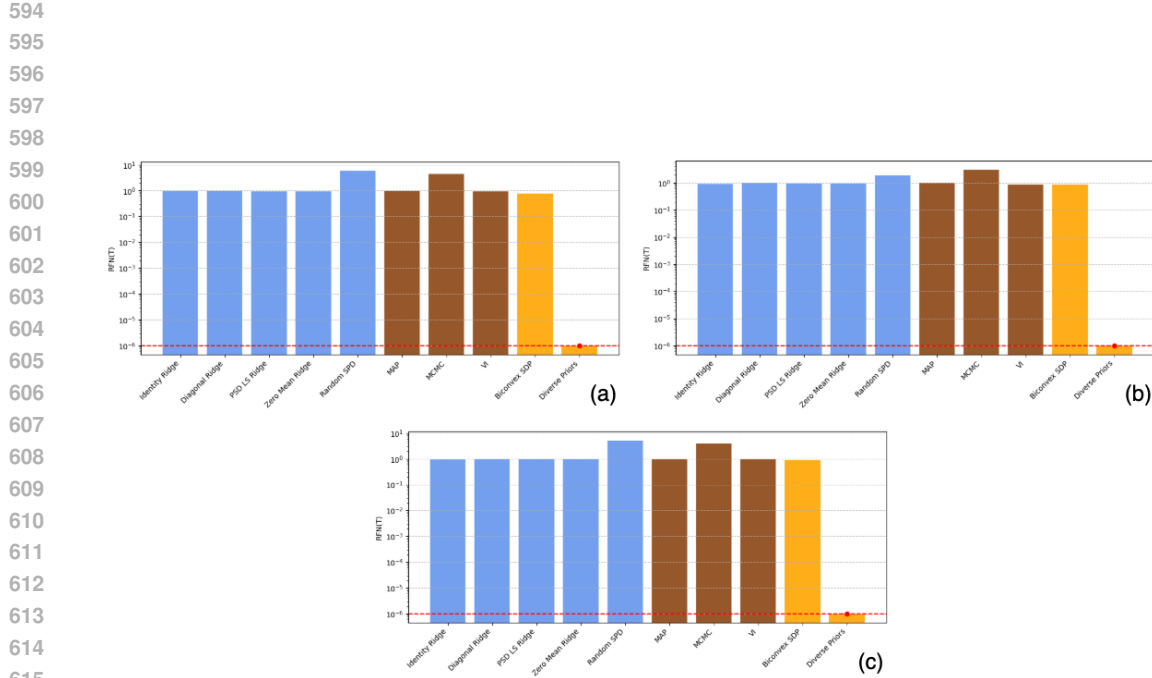


Figure 4: Comparison of $RFN(T)$ values across all techniques for the three datasets: (a) Diabetes, (b) Lung Cancer, and (c) California Housing.

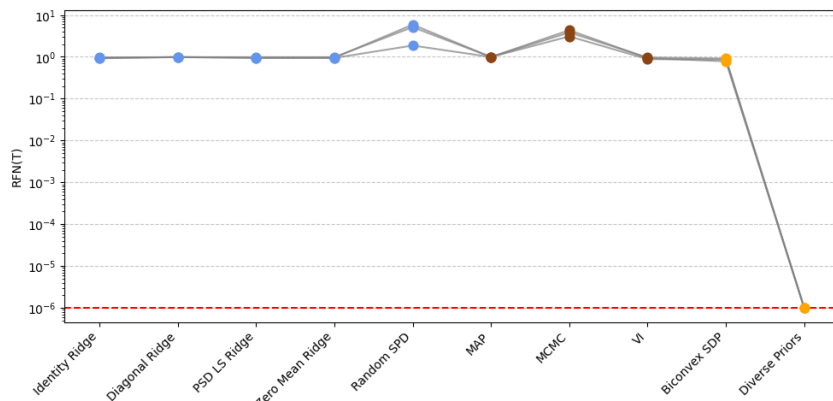


Figure 5: Comparison of $RFN(T)$ values across all techniques averaged over the three datasets.

648 A.3 TIKHONOV PRECISION PLOTS
649650 A.4 PHASE 1: GROUND TRUTH GENERATION DETAILS
651652 Fix d and sample

653 (i) $\Sigma_{\text{true}} = AA^\top + \delta I_d$, $\delta > 0$, $A \in \mathbb{R}^{d \times d}$ with i.i.d. entries, (10)
654

655 (ii) $T_{\text{true}} = \Sigma_{\text{true}}^{-1}$, $\mu_{\text{true}} \sim \mathcal{N}(0, \sigma_\mu^2 I_d)$, (11)
656

657 (iii) $\theta^* \sim \mathcal{N}(\mu_{\text{true}}, \Sigma_{\text{true}})$, (12)
658

659 (iv) $b = T_{\text{true}}(\theta^* - \mu_{\text{true}}) + \varepsilon$, $\varepsilon \sim \mathcal{N}(0, \tau_{\text{sim}}^2 I_d)$. (13)
660

661 A.5 BENCHMARKS: CONSTRAINT-BASED BAYESIAN INVERSE REGULARIZATION
662663 One approach to solving Inverse Regularization is to turn to Generative models like Bayesian In-
664 ference that assume Gaussian priors. For given $\theta^* \in \mathbb{R}^d$ obtained from a Tikhonov-regularized
665 objective, let $b \in \mathbb{R}^d$ denote the stationarity right-hand side derived from data such that $b =$
666 $-X^\top(X\theta^* - y)$. We aim to infer the prior mean $\mu \in \mathbb{R}^d$ and the Tikhonov (precision) matrix
667 T such that the (noisy) KKT stationarity holds.
668

669 The residual model can be defined as:

670
$$r = T(\theta^* - \mu) - b \in \mathbb{R}^d. \quad (14)$$

671 We assume an isotropic Gaussian noise model (with τ noise precision)

672
$$r \sim \mathcal{N}(0, \tau^2 I_d), \quad \tau > 0. \quad (15)$$

673 Equivalently, the likelihood reads

674
$$p(b | \theta^*, \mu, T, \tau) \propto \exp\left(-\frac{1}{2\tau^2} \|T(\theta^* - \mu) - b\|_2^2\right). \quad (16)$$

675 We place independent priors on μ , T , and τ :

676
$$\mu \sim \mathcal{N}(\mu_0, \Lambda_0^{-1}), \quad (17)$$

677
$$T \sim \Pi_T, \quad T \in \mathbb{S}_{\geq 0}^d, \quad (18)$$

678
$$\tau \sim \Pi_\tau, \quad \text{e.g. } \tau \sim \text{HalfNormal}(\sigma_\tau). \quad (19)$$

679 Here, μ is the prior mean vector with hyperparameters μ_0 is the prior mean center and Λ_0 is the prior
680 precision of μ , Π_T is the prior on T , supported on $\mathbb{S}_{\geq 0}^d$, and τ is the observation noise precision with
681 prior Π_τ (e.g., HalfNormal with scale σ_τ).
682683 A convenient parameterization is via the covariance $\Sigma = T^{-1}$: we draw Σ with an LKJ-Cholesky
684 prior and set $T = \Sigma^{-1}$:

685
$$\Sigma \sim \text{LKJ}(\eta, \mathbf{s}), \quad T = \Sigma^{-1}, \quad \eta > 0, \mathbf{s} = \text{diag}(\sigma_1, \dots, \sigma_d). \quad (20)$$

686 With a single constraint (equation 14), the likelihood informs T primarily along $v = \theta^* - \mu$.
687688 At the optimizer θ^* of the Tikhonov-regularized objective $\mathcal{L}(\theta) = \|y - X\theta\|^2 + (\theta - \mu)^\top T(\theta - \mu)$,
689 the stationarity condition reads
690

691
$$T(\theta^* - \mu) = -X^\top(X\theta^* - y). \quad (21)$$

692 We denote the right-hand side of equation 21 by $b \in \mathbb{R}^d$.
693694 Given (θ^*, b) , we place priors on (μ, T, τ) and write the posterior as
695

696
$$p(\mu, T, \tau | \theta^*, b) \propto \exp\left(-\frac{1}{2\tau^2} \|T(\theta^* - \mu) - b\|_2^2\right) p(\mu) p(T) p(\tau). \quad (22)$$

697 We use weakly informative priors:
698699

- $\mu_0 = 0$, $\Lambda_0 = \kappa_0 I_d$ (small κ_0),
700 • LKJ $\eta \in [1, 4]$ with scale vector \mathbf{s}
701 • and $\tau \sim \text{HalfNormal}(\sigma_\tau)$

702
703 A.6 SOLUTION STABILITY704 For numerical stability, one may model $\Sigma = AA^\top + \epsilon I_d$ with $\epsilon > 0$. To ensure feasibility, we explic-
705 itely constrain all recovered precision matrices to be positive semidefinite (PSD), which guarantees
706 valid covariance estimates. Stability is promoted by incorporating Frobenius and trace regularization
707 terms that prevent ill-conditioning and suppress extreme eigenvalues. Finally, to handle numerical
708 degeneracies during matrix inversion or eigen decomposition, we add a small jitter term ϵI (with
709 $\epsilon > 0$) to the diagonal, ensuring strict positive definiteness and stable computations throughout the
710 optimization process.

711 The entire code was written in Python 3.8 and is available in the supplementary files.

712
713
714
715
716
717
718
719
720
721
722
723
724
725
726
727
728
729
730
731
732
733
734
735
736
737
738
739
740
741
742
743
744
745
746
747
748
749
750
751
752
753
754
755